

図1 羊水中B19-DNA, Epo, Tn-T

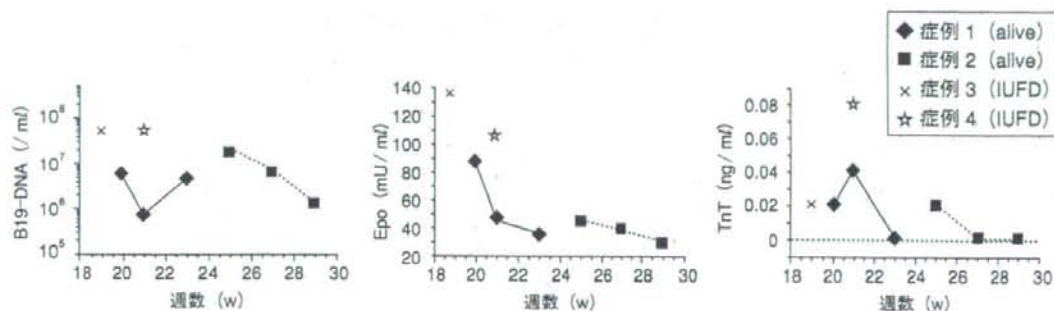


図2 胎内治療例の羊水中B19-DNA, Epo, Tn-Tの変化

B19による胎児水腫症例に対し、胎児輸血した12例中9例が生存したが、胎児輸血をしなかった26例では13例しか生存しなかったとしている ( $p < 0.05$ )。Rodisら<sup>7)</sup>はB19胎児水腫539症例による後視的研究で、胎児輸血をした症例の改善率は29%に達するが、胎児輸血をしなかった症例の30%が胎内死亡に至ったと報告している。しかしながら、胎内治療は侵襲性が強いことや、血液製剤の安全性に対する疑問などのマイナス面も依然として残っており、今後さらなる検証が求められる。

近年報告されている治療法として、胎児腹腔内免疫グロブリン注入療法が挙げられる<sup>8)</sup>。しかしながら、現時点で医学的なエビデンスが十分ではなく、治療の適応や効果は症例を集積したうえで検討する必要がある。

## 当院での試み

B19感染によって重篤な胎児水腫をきたすよう

な症例は予後が不良であり、今後胎内治療の適応の確立が必須である。しかしながら、超音波検査などの生理学的検査では貧血の程度は不明である。また、DNA検査では病勢の把握には至らない。よって、われわれは羊水中のEpoとTnTを用いて生化学的に胎児の状態を定量的に測定することを試みている。

Epoは低酸素下で神経障害を防ぐ目的で分泌される糖蛋白ホルモンであり、胎児では主に肝臓やグリア細胞で産生される<sup>9)</sup>。羊水中Epoの正常値は妊娠10週で2.0~6.3 (mU/ml)、妊娠20週で2.0~11.5 (mU/ml)、妊娠末期で4.2~19.0 (mU/ml)と報告されており、胎盤通過性はない<sup>10)</sup>。

TnTは心横紋筋を構成する蛋白であり、胎盤通過性がないことから、羊水中へのTnTの出現は心筋細胞の非可逆的障害を示す<sup>11)</sup>。

羊水中のEpoの上昇は胎児の慢性的な asphyxiaを示し、さらにその25~51%に心筋障害を合併していると報告されている<sup>12)</sup>。

胎児水腫をきたした4例を症候性胎児と定義し、胎児腹腔内免疫グロブリン注入療法(2 g/kg)を予定したが、2例は施行前に子宮内胎児死亡(intrauterine fetal death: IUFD)となった。非症候性胎児6例と併せてB19-DNA, Epo, TnTを測定し、臨床経過との関連を後方視的に検討した。

症候性胎児症例はすべてB19-DNAが $5.7 \times 10^5$  copies/ml以上であった。一方、非症候性の6例は症候性胎児症例に比べて明らかに低かった(図1)。非症候性胎児6症例の羊水中Epo値は9.1 mU/ml, 19.5 mU/ml, 18.8 mU/ml, 16.9 mU/ml, 61.3 mU/ml, 15.2 mU/mlであり、羊水中TnTは全例陰性であった(図1)。症候性胎児症例のうち、胎内治療例2例の羊水中Epo値は87.4 mU/mlから34.6 mU/ml, 44.2 mU/mlから29.3 mU/mlに減少し、以後満期で健常児を得ることができた。一方、治療前の精査中にIUFD症例となった2例の羊水中Epo値は136 mU/ml, 106 mU/mlであった。羊水中TnTに関しては4例とも陽性であった(図2)。

以上の結果から、羊水中B19-DNA, Epo, TnTは、B19感染に対する胎内治療の適応および治療効果の判定で有用となる可能性がある。

現在、B19に対する胎内治療は免疫グロブリン胎児医療研究会の作成したプロトコールに則って行われている。今後は同研究会のもとに集積されたデータをさらに解析することにより、胎内治療のさらなる発展が期待される。

## 文 献

1) Cosmi E, Mari G, Chiaie LD, et al: Noninvasive di-

- agnosis by Doppler ultrasonography of fetal anemia resulting from parvovirus infection. *Am J Obstet Gynecol* 187: 1290-1293, 2002
- 2) Brown KE, Anderson SM, Young NS: Erythrocyte P antigen: Cellular receptor for B19 parvovirus. *Science* 262: 114-117, 1993
- 3) Anderson MJ, Higgins PG, Davis LR, et al: Experimental parvoviral infection in humans. *J Infect Dis* 152: 257-265, 1985
- 4) Hayakawa H, Tara M, Niina K, et al: A clinical study of adult human parvovirus B19 infection. *Intern Med* 41: 295-299, 2002
- 5) Fairly CK, Smoleniec JS, Caul OE, et al: Observational study of effect of intrauterine transfusions on outcome of fetal hydrops after parvovirus B19. *Lancet* 346: 1335-1337, 1995
- 6) Gratacos E, Torres P, Vidal J, et al: The incidence of human parvovirus B19 infection during pregnancy and its impact on perinatal outcome. *J Infect Dis* 171: 1360-1363, 1995
- 7) Rodis JF, Quinn DL, Gary W, et al: Management and outcomes of pregnancies complicated by human B19 parvovirus infection: A prospective study. *Am J Obstet Gynecol* 163: 1168-1171, 1990
- 8) Matsuda H, Sakaguchi K, Shibasaki T, et al: Intrauterine therapy for parvovirus B19 infected symptomatic fetus using B19 IgG-rich high titer gammaglobulin. *J Perinat Med* 33: 561-563, 2005
- 9) Marti HH: Erythropoietin and the hypoxic brain. *J Exp Biol* 207: 3233-3242, 2007
- 10) Campbell J, Wathen J, Lewis M, et al: Amniotic fluid erythropoietin levels in normal and Down's syndrome pregnancies. *Eur J Obstet Gynecol* 56: 191-194, 1994
- 11) Stefanovic V, Loukovaara M: Amniotic fluid cardiac troponin T in pathological pregnancies with evidence of chorionic fetal hypoxia. *Croat Med J* 46: 801-807, 2005
- 12) Gaze D, Collinson P: Cardiac troponin determination in amniotic fluid. *Croat Med J* 46: 996-1004, 2005

## 特集

## 産婦人科感染症診療マニュアル

〔各論〕◆周産期 II. 母子感染

## 5. 風疹ウイルス

高桑好一・大木 泉・田中憲一。

新潟大学医学総合病院産婦人科。

Key Words/風疹, 胎内感染, 先天性風疹症候群

## 要旨

妊婦が妊娠初期に風疹に罹患した場合、胎児に高率に先天性風疹症候群が発症することが知られている。産科臨床の場では、妊娠初期血液検査の一つとしてほぼ全例に風疹抗体の検査が行われている。風疹の流行期でない場合、先天性風疹症候群の発症頻度は極めて低いものではあるが、風疹抗体の値によっては、妊婦の風疹罹患の可能性が完全に否定できず対応に苦慮することもある。本稿では、風疹感染、先天性風疹症候群の概要を説明し、臨床の場における実際の対応などについて解説する。

風疹 (rubella) は「三日ばしか」ともよばれ、疾患そのものは重篤なものではないが、妊婦が妊娠初期に感染した場合、児に「先天性風疹症候群」が発症する可能性が高く、周産期領域では重要な感染症である。本稿においては、風疹感染、先天性風疹症候群の概要およびその予防法などについて解説する。

## 風疹 (rubella) とは

風疹ウイルスは Togavirus 科に属する RNA ウィルスで、血清学的には亜型のない単一のウィルスである。風疹は風疹ウイルス感染による

発疹性疾患であり、発熱、発疹、リンパ節腫脹を特徴とする。潜伏期は 16～18 日で、小児では鼻汁、下痢などに引き続き発疹が認められることが多いが、成人では微熱ののち、食欲不振、倦怠感、結膜炎、上気道炎様症状が認められ、頭、耳介後部などのリンパ節腫脹が認められ、その後発疹が認められることが多い。上気道から分泌されたウイルスによる飛沫感染形式をとるが、感染力は麻疹、水痘などに比べ弱い。

風疹の疫学についてであるが、従来は 2～3 年の周期で流行し、10 年ごとに大流行がみられていた。ここ 25 年ほどの間では、1982 年、1987 年、1992 年に大きい流行がみられたが、次第にその発生数および流行の規模は縮小しつ



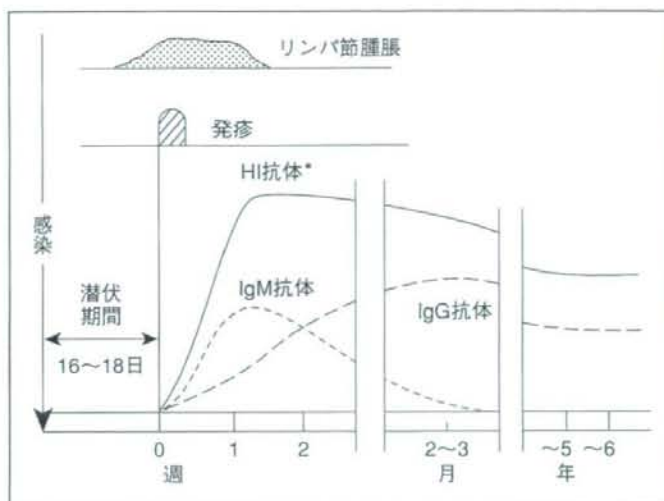


図1 風疹感染の経過と抗体の推移

\* HI抗体：ピーク時は256倍～2048倍，時間の経過とともに32倍から128倍で安定（ただし，時間が経過してからの抗体価は幅がある）

つある。

風疹の診断は，上記の発熱，発疹，リンパ節腫脹の3主徴に基づくが，他の発疹性疾患との鑑別のため，血清学的診断が重要である。血清学的診断として通常用いられるものは，風疹HI (hemagglutination inhibition, 赤血球凝集抑制) 抗体，および酵素免疫測定法 (ELISA) により測定されるグロブリン別風疹抗体すなわち，風疹IgG抗体，IgM抗体である。風疹感染に伴うこれらの抗体の推移を図1に示した。

発疹出現後48時間以内に抗体価が上昇し，HI抗体価は発疹発現後ほぼ1週間でピークに達する。これと同時期に風疹IgM抗体が上昇し4～5週間で低下するため，IgM抗体が陽性である場合，最近の風疹感染の可能性があり，診断上有用とされてきた。ただし，風疹IgM抗体が長期にわたり陽性を示すこともあり注意が必要であるが，これについては後述する。風疹IgG抗体は，IgM抗体が低下したのち上昇するため，IgG抗体が陽性，IgM抗体が陰性であれば最近の感染は否定的となる。

妊娠と風疹感染の最大の問題は，先天性風疹

症候群であり，以下にそのことについて解説する。

## 先天性風疹症候群

### 1. 症状および感染時期と胎児異常

妊娠初期に風疹に罹患した場合，児の先天性風疹症候群 (congenital rubella syndrome: CRS) 発症のリスクが高まる。発症率についての報告には幅があるが，高い方の報告では妊娠第1カ月の風疹感染で約60%，第2カ月で80%，第3カ月で約50%，第4カ月で約20%，第5カ月では約15%などという報告がなされている<sup>2)</sup>。CRSの3大症状は先天性心疾患，難聴，白内障である。このうち，白内障は妊娠3カ月以内，先天性心疾患は4カ月以内の風疹感染で発症することが知られているが，難聴は4カ月以後でも発症する可能性がある<sup>2)</sup>。3大症状以外に網膜症，肝脾腫，血小板減少，糖尿病，発育遅滞，精神発達遅滞，小眼球症など多様な症状が認められることがある。

## 2. 先天性風疹症候群の診断

出生した児に先天性心疾患、難聴、白内障などのCRSを疑わせる症状が認められる場合には、ウイルス学的検査あるいは免疫学的検査により診断を行う。表1にその診断基準を示した<sup>3)</sup>。CRSは全例報告の必要があり、CRSの診断を行った場合には届け出を行う。

## 3. 先天性風疹症候群の予防

予防で重要なことは、妊娠可能年齢の女性が十分高い風疹抗体価を保有することである。わが国では平成6年以前は中学生の女子のみが風疹ワクチン接種の対象であったが、平成6年の予防接種法改正により、対象が生後12カ月以上～90カ月未満の男女(標準は生後12カ月以上～36カ月以下)とされた。その後さらに改正され2006年からは、生後12～24カ月(第1期)および就学前1年間(第2期)の男女となっている。ただし、平成15年の推計では20歳台、30歳台の女性70万人が風疹抗体陰性で

あることが指摘されている<sup>4)</sup>、すでに自然感染により免疫を獲得していることが明らかな場合以外は、風疹ワクチンによる能動免疫により風疹抗体を獲得せしめることが重要である(ただし、風疹ワクチンは弱毒生ワクチンであり、妊娠中のワクチン接種は避ける)。

## 4. 妊娠中に風疹罹患が考慮された場合の対応

2004年、それまでCRSの発症が年間1例程度であったものが半年で5例報告されたため、厚生労働省研究班が「風疹流行および先天性風疹症候群の発生抑制に関する緊急提言」を行った<sup>5)</sup>。その内容は以下のとおりである。

現状でも妊娠初期検査としてほぼ全例に風疹抗体検査が実施されていると思われるが、同提言では、妊娠初期検査の一環として風疹抗体(HI抗体)を検査することを前提としている。そのうえで問診の重要性を指摘しており、「妊娠中の発疹の有無」「風疹患者との濃厚な接触

表1 先天性風疹症候群報告のための基準  
(改正感染症法, 2003年11月)

<p>診断した医師の判断により、症状や所見から当該疾患が疑われ、かつ、以下の1)と2)の基準を両方とも満たすもの</p> <p>1) 臨床症状による基準</p> <p>「Aから2項目以上」または「Aから1つと、Bから2つ以上」もしくは「Aの(2)または(3)と、B(1)」</p> <p>A. (1) 先天性白内障、または緑内障</p> <p>(2) 先天性心疾患(動脈管開存、肺動脈狭窄、心室中隔欠損、心房中隔欠損など)</p> <p>(3) 感音性難聴</p> <p>B. (1) 網膜症</p> <p>(2) 骨端発育障害(X線診断によるもの)</p> <p>(3) 低出生時体重</p> <p>(4) 血小板減少性紫斑病(新生児期のもの)</p> <p>(5) 肝脾腫</p> <p>2) 病原体診断等による基準</p> <p>以下のいずれかの一つを満たし、出生後の風疹感染を除外できるもの</p> <p>1. 風疹ウイルスの分離陽性、またはウイルス遺伝子の検出</p> <p>例: RT-PCR法など</p> <p>2. 血清中に風疹特異的IgM抗体の存在</p> <p>3. 血清中の風疹HI価が移行抗体の推移から予想される値を高く越えて持続(出生児の風疹HI価が、月あたり1/2の低下率で低下していない)</p>
---

表2 妊娠初期検査における風疹抗体価による対応  
(問診により風疹感染を考慮させる状況にない場合)

風疹抗体価	取り扱い
陰性または16倍以下	妊娠中の注意指導 人込みや子どもの多い場所を避ける 風疹患者のいる場所を避ける 夫、子どもおよび同居家族へのワクチン接種推奨 分娩後早期のワクチン接種の推奨
32～128倍	以後の妊娠の経過中、以下に該当するか 妊娠中の発疹 風疹患者との濃厚な接触 なければ終了 あれば「256倍以上」の取り扱いへ
256倍以上	再度血清 HI および風疹 IgM を測定 HI 不変かつ IgM 陰性：終了 HI が4倍以上の上昇または IgM 陽性 各地区相談窓口（2次施設）へ相談

の有無」について聴取することを勧めている。問診で該当項目がない場合、風疹抗体価により表2のような対応を行う。HI抗体価が陰性あるいは16倍以下の場合には、風疹ウイルスに対する免疫がないかあるいは不十分と判断して対応する。HI抗体価が32～128倍の場合適度な免疫を保有していると判断し、256倍以上では最近の風疹感染の可能性も考慮し対応する。ただし、256倍以上であるとしても風疹感染である可能性は極めて低く、妊婦に過剰な不安を抱かせないことが重要である。

問診で該当項目がある場合には、ペア血清で風疹 HI 抗体および風疹 IgM 抗体を測定する。HI 抗体が陰性あるいは16倍以下の場合には表2の項目に従う。ペア血清検査で HI 不変かつ IgM 陰性の場合には終了とし HI が4倍以上の上昇を示すが、IgM が陽性の場合には各地区ブロックごとの相談窓口（二次施設）へ相談することを勧めている（相談窓口である二次施設については文献5）を参照されたい）。

この提言では、風疹感染を考慮すべき状況で風疹 IgM 抗体の測定を行い、陽性の場合には二次施設への相談を推奨している。しかしながら、

風疹 IgM 抗体が弱陽性を示すことが時にあり、その場合（多くの医療施設にとって）遠隔地である二次施設へ紹介すべきか否か迷うところである。次項ではこの点について述べる。

#### 5. 風疹 HI 抗体高値、IgM 抗体弱陽性例に関する対応の参考として

奥田らは風疹 IgM 抗体は基本的には風疹感染後2～3カ月で陰性となるよう cut off 値が設定されているものの、低いレベルの陽性が3年以上持続する例も存在することから、IgM が陽性であっても直ちに最近の感染とはいえないと指摘している。このような状況に関連して、参考として当科で遺伝相談を行った症例を提示する。

症例は20歳台、前医で双胎妊娠の診断を受け、妊娠初期検査で風疹 HI 抗体価が512倍であった。グロブリン別抗体を検査したところ、風疹 IgG 抗体が128以上（cut off 値：4.0）、風疹 IgM 抗体が2.08（cut off 値：1.2）であった。妊娠後の発疹の有無、風疹患者との濃厚な接触の有無などについて聴取したが該当しなかった。約1カ月後に再検したところ、風疹 IgG 抗体128以上、風疹 IgM 抗体1.92とほぼ不変で



あった。これに対し、風疹 HI 抗体高値、IgM 抗体陽性であるものの風疹感染を考慮させるエピソードはなく、感染の可能性が極めて低い(0ではないが)ことを説明し、妊娠継続となった。妊娠 34 週で分娩となり、両児に関して NICU で風疹感染についての精査も実施したが、CRS は否定された。

日本産科婦人科学会編集の『産婦人科診療ガイドライン—産科編 2008』では風疹 IgM 抗体に関して「Persistent IgM」という概念を指摘しており、コンセンサスを得たものではないが、その基準として、①低レベル、②1～2カ月後の再検でもほぼ同じ値で検出、③高い IgG 抗体価、を提示している<sup>6)</sup>。本症例はこの概念に合致する症例と考えられるが、風疹感染の可能性が否定しきれない場合には、二次施設への相談、情報交換を考慮することが重要である。

#### 6. 風疹罹患に関する胎内診断

妊娠初期の風疹感染の可能性が否定しきれない場合には、上述のように二次施設への相談、紹介などを行うこととなる。胎児が感染したか否かは、胎盤絨毛、胎児血、羊水などの胎児由来組織中に風疹ウイルス遺伝子を検出することで判定されるが、風疹ウイルス RNA を RT-PCR (reverse transcriptase-polymerase chain reaction) 法で増幅して検出する方法が応用される。これについて種村は、羊水では検出率がやや低く偽陰性例が存在すること、高感度で結果を得るには絨毛あるいは胎児血を用いることが望ましいことを報告している。また、RT-PCR で陽性であっても CRS が発症するとは限らず、十分なカウンセリングが必要であることを指摘している<sup>7)</sup>。

なっているが、妊娠初期に風疹抗体の検査を行い高値である場合、医療者、患者ともに過剰な不安を抱くことがある。また、風疹ワクチン接種に関する法改定のはざまとなった年代(1982～1987年生まれ)の婦人で風疹抗体陽性率が低いことが指摘されており、妊娠中の風疹感染の増加が危惧されている。産婦人科医としては、妊娠可能年齢にある女性に対し妊娠成立前の風疹抗体獲得の重要性をアピールし、CRS が根絶されるよう努力することが重要であると考えられる。

## 文 献

- 1) 砂川慶介：ウイルス感染症 皮膚症状を伴うウイルス感染症 風疹。日本臨床 43:650-652, 1985.
- 2) 干場 勉：女性診療のための感染症のすべて。妊婦と風疹。産婦治療 90:587-591, 2005.
- 3) 国立感染症研究所感染症情報センター：風疹の現状と今後の風疹対策について。  
(<http://idsc.nih.go.jp/disease/rubella/rubella.html>)
- 4) 奥田美加, 高橋恒男, 平原史樹：母子感染とその対策 妊婦における風疹抗体価。産婦治療 95:55-60, 2007.
- 5) 厚生科学研究費補助金, 新興・再興感染症研究事業分担研究班：風疹流行および先天性風疹症候群の発生抑制に関する緊急提言。  
(<http://idsc.nih.go.jp/disease/rubella/rec200408.pdf>)
- 6) 日産婦会, 日本産婦人科医会(編)：産婦人科診療ガイドライン—産科編 2008 CQ605「妊婦における風疹罹患の診断と対応は？」154-156, 日産婦会事務局, 2008.
- 7) 種村光代：周産期感染症の現在, 先天異常児と妊娠中の感染症。化学療法領域, 17:1066-1073, 2001.

#### 著者連絡先

(〒951-8510)  
新潟市中央区旭町通 1-757  
新潟大学医歯学総合病院産婦人科  
高桑好一

## おわりに

近年、CRS 発症の頻度は極めて低いものと

## Intracellular Efavirenz Levels in Peripheral Blood Mononuclear Cells from Human Immunodeficiency Virus-Infected Individuals<sup>∇</sup>

Rie Tanaka,<sup>1</sup> Hideji Hanabusa,<sup>2</sup> Ei Kinai,<sup>2</sup> Naoki Hasegawa,<sup>1</sup> Masayoshi Negishi,<sup>1</sup> and Shingo Kato<sup>1\*</sup>

Keio University School of Medicine<sup>1</sup> and Ogikubo Hospital,<sup>2</sup> Tokyo, Japan

Received 27 December 2006/Returned for modification 15 March 2007/Accepted 28 November 2007

**We describe a novel method for isolating plasma-free peripheral blood mononuclear cells retaining intracellular efavirenz. Quantification of efavirenz in 13 human immunodeficiency virus-infected patients by liquid chromatography-tandem mass spectrometry showed a higher correlation of intracellular levels with unbound plasma levels (accumulation ratio, 1,190) than with total plasma levels.**

Efavirenz, a nonnucleoside reverse transcriptase inhibitor, is a major component of current antiretroviral therapy for human immunodeficiency virus (HIV) type 1 infection. Several studies supported the idea of the usefulness of therapeutic drug monitoring of efavirenz, because viral suppression and adverse effects are associated with efavirenz levels in plasma (3, 9). Given that efavirenz exerts inhibitory activity with respect to reverse transcriptase and may interact with cellular enzymes within the cell, it is likely that intracellular levels are more relevant to the clinical outcome than plasma levels (10). Intracellular efavirenz levels have been explored using similar procedures, which consisted of preparation of peripheral blood mononuclear cells (PBMCs) by Ficoll density gradient centrifugation and cell washing with ice-cold phosphate buffered saline (PBS) (1, 2, 10). During our preliminary experiments, it was observed that efavirenz in PBS strongly stuck to the surface of plastic microcentrifuge tubes and was difficult to wash away with PBS. Such a property of adherence of efavirenz may have affected measurements of intracellular quantities in the previous protocols.

First, the efflux rate of efavirenz from cells was studied. PBMCs isolated from a healthy donor by use of Ficoll-Paque Plus solution (GE Healthcare, Piscataway, NJ) were incubated in 1  $\mu$ M efavirenz in serum-free VP-SFM medium (Invitrogen, Carlsbad, CA) at 37°C for 1 h and then transferred to drug-free medium and incubated at either 4°C or 37°C for up to 20 min. Three aliquots of 10<sup>6</sup> cells were taken at each time point, and the efavirenz contained in each aliquot was extracted with 80% methanol and quantified by liquid chromatography-tandem mass spectrometry (LC-MS/MS) with a high-performance LC system (Agilent 1100 Series; Agilent, Palo Alto, CA) and a tandem mass spectrometer (API QStar Pulsar I; Applied Biosystems, Foster City, CA) using electrospray ionization in which an *m/z* transition of 333 to 272 atomic mass units for (M+NH<sub>4</sub>)<sup>+</sup> precursor ions of efavirenz was used. As shown in Fig. 1, the intracellular efavirenz concentration declined within 5 min at either 37°C or 4°C to a level near the background level. This result poses another question about the previous

isolation procedures used for PBMCs, because they were based on the assumption that drug efflux produced during washing procedure is suppressed by the use of ice-cold PBS. This result, taken together with those demonstrating the highly lipophilic property of efavirenz, suggests that intracellular efavirenz is eluted from the cells and adsorbed to the surface of plastic vessels during cell washing. To examine this hypothesis we compared quantifications of levels of efavirenz in PBMCs by two different isolation protocols: one used the same tube during washing, and the other used new tubes in each washing (Table 1). Transfer of cell suspension to a new tube each time reduced the efavirenz quantity remarkably compared with the use of the same tube throughout washing. These results suggest that the drug exudes from cells during cell washing and that the drug present in residual plasma was not washed away in studies employing the previously used procedures.

Thus, we decided to develop a new method for isolation of PBMCs (Fig. 2). The method consists of three steps: banding of PBMCs at the bottom of the plasma layer but not in the Ficoll-Paque solution by a relatively short centrifugation time; washing of PBMCs with concurrently prepared plasma of the same patient; and separation of PBMCs from the plasma by centrifugation through silicone oil (supplemented with 8% *n*-hexadecane) in a "double tube." By this method, efavirenz in PBMCs are kept equilibrated with the efavirenz in plasma until

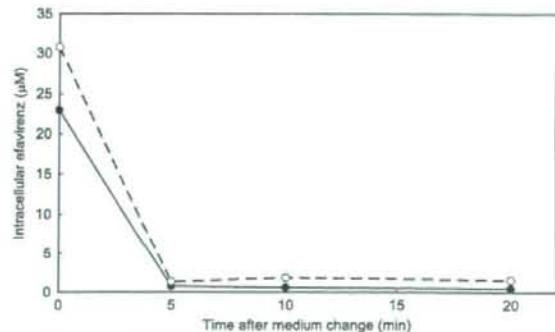


FIG. 1. Efflux of efavirenz from preequilibrated PBMCs following incubation in drug-free medium at 37°C (closed circles) and 4°C (open circles).

\* Corresponding author. Mailing address: Department of Microbiology and Immunology, Keio University School of Medicine, 35 Shinanomachi, Shinjuku-ku, Tokyo 160-8582, Japan. Phone: 81 3 5363 3769. Fax: 81 3 5360 1508. E-mail: skato@sc.itc.keio.ac.jp.

<sup>∇</sup> Published ahead of print on 10 December 2007.



TABLE 1. Quantification of efavirenz in PBMCs isolated by the present method and a previously reported method<sup>a</sup>

Source	Intracellular efavirenz concn <sup>b</sup> ( $\mu\text{M}$ )		
	Previous method with one tube <sup>c</sup>	Previous method with new tubes <sup>d</sup>	Present method <sup>e</sup>
Spiked donor blood <sup>f</sup>	110 $\pm$ 19	4.6 $\pm$ 1.7	97 $\pm$ 17
Patient 1	Not assayed	3.8 $\pm$ 1.3	63 $\pm$ 24
Patient 2	Not assayed	1.1 $\pm$ 0.3	71 $\pm$ 11

<sup>a</sup> The method reported by Almond et al. (1) was used for isolation of PBMCs for comparison with the present method.

<sup>b</sup> Efavirenz was quantified by LC-MS/MS. Intracellular concentrations were calculated, taking 0.25 pl as the volume of a single cell (5). Data are expressed as means  $\pm$  standard deviations ( $n = 3$ ).

<sup>c</sup> Washing of PBMCs in ice-cold PBS was carried out three times in the same microcentrifuge tube.

<sup>d</sup> Suspension of PBMCs in ice-cold PBS was transferred into a new microcentrifuge tube for centrifugation before each of three washings.

<sup>e</sup> Intracellular efavirenz concentrations were determined as described in the legend to Fig. 2.

<sup>f</sup> HIV-uninfected donor blood was spiked with efavirenz at 10  $\mu\text{M}$ .

PBMCs are separated from the plasma. The use of a "double tube" in centrifugation prevents plasma from contaminating the surface of an outer microcentrifuge tube and thus from getting into the extract of PBMCs.

By using this method, we studied the dependence of intracellular efavirenz levels on the concentration of plasma in medium containing efavirenz at 10  $\mu\text{M}$ . Efavirenz not bound by protein was obtained by use of a Centrifree micropartition device (Centrifree, Billerica, MA). The intracellular efavirenz

concentration decreased with an increase in the plasma concentration (Fig. 3A) and was proportional to the unbound efavirenz concentration in medium, with a mean intracellular accumulation ratio of 970 (Fig. 3B). These results show that the major determinant of intercellular efavirenz levels is extracellular unbound levels but not total extracellular levels, which agrees with the pharmacological idea that only unbound drug is able to enter the cell.

Next, the relationships between total plasma, unbound plasma, and intracellular efavirenz concentrations were studied using samples from 13 patients receiving antiretroviral agents containing efavirenz in Keio University Hospital (Tokyo, Japan). The patients provided written informed consent for the study, which was approved by the local ethics committee. The median duration of treatment was 15 months, with a range from 1 to 65 months. Concurrent drugs used for treatment were zidovudine and lamivudine (3TC) for four patients, stavudine and 3TC for five, tenofovir disoproxil fumarate and emtricitabine for three, and tenofovir disoproxil fumarate and 3TC for one. All patients were Japanese males and exhibited no biochemical evidence of impairment of the liver or kidney. Although there were significant associations between total and unbound plasma levels (Spearman's rank correlation coefficient [ $r_s$ ] = 0.66;  $P = 0.021$ ) (Fig. 4A) and between total plasma and intracellular levels ( $r_s = 0.66$ ;  $P = 0.021$ ) (Fig. 4B), a stronger correlation was observed between unbound plasma and intracellular levels ( $r_s = 0.76$ ;  $P = 0.0082$ ) (Fig. 4C), with a mean accumulation ratio of 1,190.

The results presented above are contrasted with the results

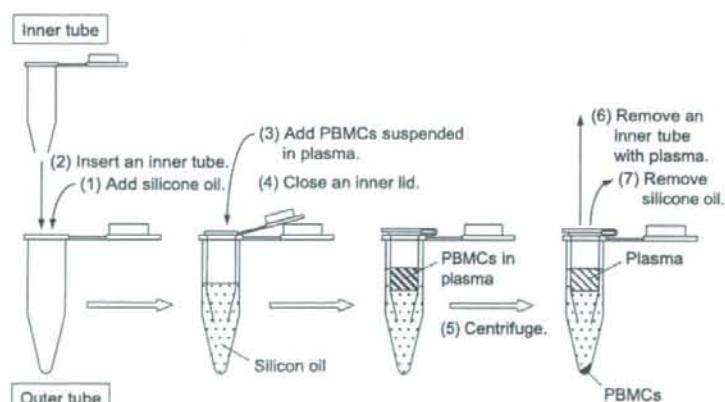


FIG. 2. Preparation of PBMCs for intracellular efavirenz quantification. Anticoagulated blood (1 ml) was layered on 800  $\mu\text{l}$  of a Ficoll-Paque Plus solution (GE Healthcare, Piscataway, NJ) and centrifuged at  $180 \times g$  for 10 min. After centrifugation, PBMCs which formed a layer at the boundary between plasma and Ficoll-Paque Plus solution were collected and centrifuged at  $320 \times g$  for 2 min. Precipitated PBMCs were washed in 100  $\mu\text{l}$  of plasma prepared from the same blood and centrifuged at  $500 \times g$  for 2 min. PBMCs were separated from plasma as follows: (i) a mixture of silicone oil (catalog no. SH-550; Nacalai, Kyoto, Japan) and *n*-hexadecane (Nacalai) (800  $\mu\text{l}$ ; 92:8 [vol/vol]) was added into an outer tube (1.5-ml microcentrifuge tube); (ii) an inner tube (made from a 0.5-ml microcentrifuge tube) with a hole at the bottom was sunk in silicone oil in the outer tube; (iii) PBMCs suspended in 100  $\mu\text{l}$  of plasma were layered on silicone oil in the inner tube; (iv) the lid of the inner tube was pressed down; (v) an assembled "double tube" was centrifuged at  $16,000 \times g$  for 1 min, thereby precipitating PBMCs quickly to the bottom of the outer tube; (vi) the inner tube containing plasma and silicone oil was removed, with the lid kept closed to prevent plasma falling into the outer tube; and (vii) silicone oil was removed while leaving pelleted PBMCs in place and then the remaining silicone oil on the tube surface was removed after a brief centrifugation. Pelleted PBMCs were suspended in 30  $\mu\text{l}$  of water, and immediately 10  $\mu\text{l}$  of the suspension was used for determination of cell numbers with a cell counter (Celltac; Nihon Kohden, Tokyo, Japan); note that suspending cells in PBS is not recommended, because the presence of phosphate ions in samples affects ionization of molecules in mass spectrometry and sometimes causes severe troubles to the machine. To the remaining cell suspension, 80  $\mu\text{l}$  of methanol was added, and efavirenz was quantified by LC-MS/MS.

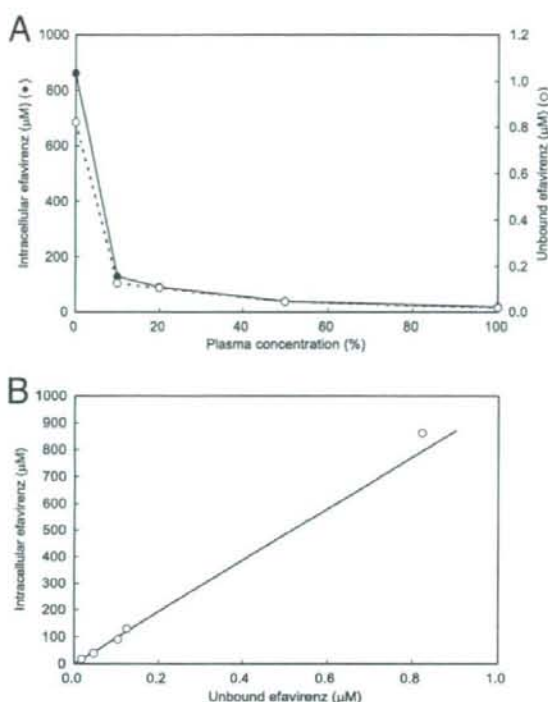


FIG. 3. (A) Dependence of unbound efavirenz and intracellular efavirenz levels on plasma content (expressed in percentages) in medium containing efavirenz at 10  $\mu\text{M}$ . (B) Relationship between unbound and intracellular efavirenz concentrations as deduced from the data presented in panel A.

of previous studies (1, 10) and demonstrate that intracellular efavirenz levels are not correlated with unbound plasma levels but are significantly correlated with total plasma levels. They indicate that total plasma efavirenz concentrations may be good surrogate markers for intracellular concentrations and that binding of efavirenz to plasma protein may be linked to its binding to unknown materials in cells. It should be noted that these studies used similar methods for isolation of PBMCs in which PBMC extract is, as argued above, apt to be contaminated with plasma efavirenz. If such contamination occurred in their studies, it would be inevitable that a stronger correlation would be observed between total plasma and intracellular efavirenz levels.

Efavirenz was highly accumulated in resting PBMCs. This may have been due to the binding to cellular protein or membrane because of its high lipophilicity ( $\log P = 5.4$ ). Efavirenz bound to cellular components is unlikely to play a direct role in inhibition of reverse transcriptase activity. To study further the biological significance of intracellular drugs, new technologies for quantifying intracellular unbound drug and for identifying intracellular drug localization are required.

Most protease inhibitors also have the properties of rapid excretion from cells and high lipophilicity (4, 8). It may be necessary to examine whether the procedures for intracellular

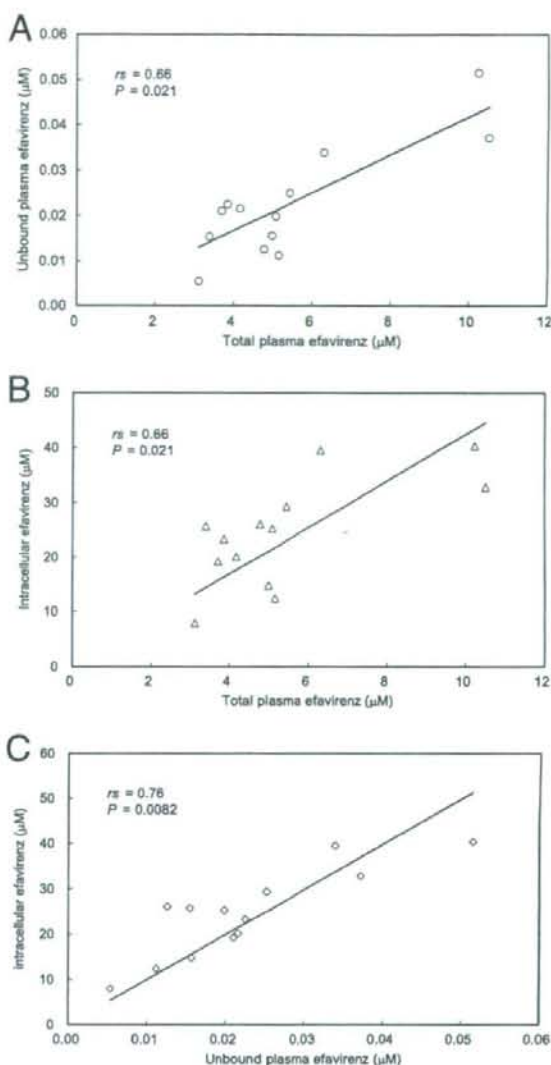


FIG. 4. Relationship between total plasma efavirenz and unbound plasma concentrations (A), total plasma and intracellular concentrations (B), and unbound plasma and intracellular concentrations (C) in samples from 13 patients receiving antiretroviral therapy that included efavirenz treatment. Data were analyzed by Spearman rank correlation.

quantification of these agents (6, 7) suffer from the possible artifacts suggested for efavirenz in this study.

In conclusion, we have developed an intracellular efavirenz quantification method which overcomes spontaneous drug elution from cells and contamination with drug-containing plasma. The present method may be a useful tool for elucidating the therapeutic relevance of intracellular levels of efavirenz.

This study was supported by grants from the Ministry of Health, Labor and Welfare of Japan.



We thank Toshio Fukazawa for critical reading of the manuscript and gratefully acknowledge all the patients who participated in this trial.

## REFERENCES

1. Almond, L. M., P. G. Hoggard, D. Edirisinghe, S. H. Khoo, and D. J. Back. 2005. Intracellular and plasma pharmacokinetics of efavirenz in HIV-infected individuals. *J. Antimicrob. Chemother.* **56**:738–744.
2. Colombo, S., A. Beguin, A. Telenti, J. Biollaz, T. Buclin, B. Rochat, and L. A. Decosterd. 2005. Intracellular measurements of anti-HIV drugs indinavir, amprenavir, saquinavir, ritonavir, nelfinavir, lopinavir, atazanavir, efavirenz and nevirapine in peripheral blood mononuclear cells by liquid chromatography coupled to tandem mass spectrometry. *J. Chromatogr. B Analyt. Technol. Biomed. Life Sci.* **819**:259–276.
3. Csajka, C., C. Marzolini, K. Fattinger, L. A. Decosterd, J. Fellay, A. Telenti, J. Biollaz, and T. Buclin. 2003. Population pharmacokinetics and effects of efavirenz in patients with human immunodeficiency virus infection. *Clin. Pharmacol. Ther.* **73**:20–30.
4. Ford, J., S. H. Khoo, and D. J. Back. 2004. The intracellular pharmacology of antiretroviral protease inhibitors. *J. Antimicrob. Chemother.* **54**:982–990.
5. Gao, W.-Y., A. Cara, R. C. Gallo, and F. Lori. 1993. Low levels of deoxynucleotides in peripheral blood lymphocytes: a strategy to inhibit human immunodeficiency virus type 1 replication. *Proc. Natl. Acad. Sci. USA* **90**:8925–8928.
6. Jones, K., P. G. Bray, S. H. Khoo, R. A. Davey, E. R. Meaden, S. A. Ward, and D. J. Back. 2001. P-glycoprotein and transporter MRP1 reduce HIV protease inhibitor uptake in CD4 cells: potential for accelerated viral drug resistance? *AIDS* **15**:1353–1358.
7. Jones, K., P. G. Hoggard, S. D. Sales, S. Khoo, R. Davey, and D. J. Back. 2001. Differences in the intracellular accumulation of HIV protease inhibitors *in vitro* and the effect of active transport. *AIDS* **15**:675–681.
8. Khoo, S. H., P. G. Hoggard, I. Williams, E. R. Meaden, P. Newton, E. G. Wilkins, A. Smith, J. F. Tjia, J. Lloyd, K. Jones, N. Beeching, P. Carey, B. Peters, and D. J. Back. 2002. Intracellular accumulation of human immunodeficiency virus protease inhibitors. *Antimicrob. Agents Chemother.* **46**:3228–3235.
9. Marzolini, C., A. Telenti, L. A. Decosterd, G. Greub, J. Biollaz, and T. Buclin. 2001. Efavirenz plasma levels can predict treatment failure and central nervous system side effects in HIV-1-infected patients. *AIDS* **15**:71–75.
10. Rotger, M., S. Colombo, H. Furrer, G. Bleiber, T. Buclin, B. L. Lee, O. Keiser, J. Biollaz, L. Decosterd, A. Telenti, and the Swiss HIV Cohort Study. 2005. Influence of *CYP2B6* polymorphism on plasma and intracellular concentrations and toxicity of efavirenz and nevirapine in HIV-infected patients. *Pharmacogenet. Genomics* **15**:1–5.

# Buoyant density and sedimentation dynamics of HIV-1 in two density-gradient media for semen processing

Naoaki Kuji, M.D., Ph.D.,<sup>a</sup> Tsuyoshi Yoshii, M.D., Ph.D.,<sup>a</sup> Toshio Hamatani, M.D., Ph.D.,<sup>a</sup> Hideji Hanabusa, M.D., Ph.D.,<sup>c</sup> Yasunori Yoshimura, M.D., Ph.D.,<sup>a</sup> and Shingo Kato, Ph.D.<sup>b</sup>

<sup>a</sup> Department of Obstetrics and Gynecology and <sup>b</sup> Department of Microbiology and Immunology, Keio University School of Medicine; and <sup>c</sup> Department of Hematology, Ogikubo Hospital, Tokyo, Japan

**Objective:** To compare buoyant density and sedimentation kinetics of human immunodeficiency virus 1 (HIV-1) in two sperm-washing media, Percoll and Pureception.

**Design:** Laboratory study.

**Setting:** University hospital.

**Patient(s):** None.

**Intervention(s):** Buoyant density and sedimentation kinetics of HIV-1 particles (MOLT-4/LAI strain) were measured in Percoll and Pureception using isopycnic ultracentrifugation and continuous-density-gradient centrifugation.

**Main Outcome Measure(s):** The HIV-1 particles were detected and semiquantified using a reverse transcription polymerase chain reaction (RT-PCR) for HIV-1 RNA.

**Result(s):** Calculated buoyant density of HIV-1 was approximately 1.042 in both media in isopycnic centrifugation. However, most HIV-1 particles were found in fractions with specific gravity less than 1.04 in both media, even after 40 minutes of density-gradient centrifugation at 1,600 g. Small viral accumulations were observed at the bottom of the tube in Pureception density gradients.

**Conclusion(s):** Although we found very high efficiency of HIV-1 removal using density-gradient centrifugation, a minute quantity of virus was found at the bottom of the gradient tube when Pureception was used as the medium. (Fertil Steril® 2008;90:1983-7. ©2008 by American Society for Reproductive Medicine.)

**Key Words:** Sperm, Percoll, Pureception, density-gradient centrifugation, HIV-1, isopycnic centrifugation

Transmission of human immunodeficiency virus type 1 (HIV-1) through semen is widely recognized. Many studies have demonstrated that HIV-1 exists both as free virus in the seminal plasma and as cell-associated virus in semen (1-8). Sperm preparation techniques originally developed to separate the fraction containing highly motile spermatozoa from that of seminal plasma and nonmotile cells have been reported to reduce HIV-1 RNA and proviral DNA to undetectable concentrations (9, 10).

Increasingly, serodiscordant couples with an HIV-1-positive husband and an HIV-1-negative wife are requesting insemination techniques for avoiding risk of transmission to the female partner and to offspring (11). Intrauterine insemination (IUI), in vitro fertilization (IVF), and intracytoplasmic sperm injection (ICSI) after sperm preparation by techniques commonly referred to as "sperm washing" have been suggested as ways to reduce likelihood of transmission of HIV-1. Numerous pregnancy successes without HIV-1 seroconversions have been reported (12-14).

Sperm washing as the first step of the virus elimination procedure has used density-gradient centrifugation. Because

HIV-1 infection is believed to worsen the condition of sperm, men with chronic HIV-1 infection often have abnormal semen profiles (15). An optimal washing method would maximize recovery of spermatozoa without decreasing viral removal efficacy. To the best of our knowledge, however, precise reliable data have not been obtained concerning buoyant density or sedimentation kinetics of HIV-1 in density-gradient media such as polyvinylpyrrolidone (PVP)-coated colloid-silica gel (Percoll) or silane-coated colloid-silica gel (Pureception). The latter medium has been used increasingly in place of Percoll.

In the present study, we determined the buoyant density of free HIV-1 in each of two sperm-washing media, Percoll and Pureception, using a highly sensitive nested competitive reverse transcription polymerase chain reaction (RT-PCR) technique that we established previously (10). Sedimentation dynamics in continuous density gradients using these two media also were investigated.

## MATERIALS AND METHODS

### Reagents

Each concentration of Pureception solution was prepared by diluting 90% Pureception with sperm-washing medium (both from Sage In Vitro Fertilization, Pasadena, CA). Each concentration of Percoll solution was prepared by diluting 80% Percoll according to the method of Kaneko et al. (16), using 10 mmol/L HEPES-buffered Hanks solution

Received May 30, 2007; revised and accepted September 13, 2007.

Supported in part by a Grant-in-Aid for Scientific Research from the Ministry of Education, Science and Culture of Japan (no. 12671629).

Reprint requests: Naoaki Kuji, M.D., Ph.D., Department of Obstetrics and Gynecology, School of Medicine, Keio University, 35 Shinanomachi, Shinjuku-ku, Tokyo 160-8582, Japan (FAX: +81-3-3226-1667; E-mail: naoaki@sc.itc.keio.ac.jp).

0015-0282/08/\$34.00

doi:10.1016/j.fertnstert.2007.09.025

Fertility and Sterility® Vol. 90, No. 5, November 2008

1983

Copyright ©2008 American Society for Reproductive Medicine, Published by Elsevier Inc.



(pH 7.4) including 4.0 mg/mL human serum albumin and antibiotics (0.14 mg/mL latamoxef sodium and 0.11 mg/mL ampicillin).

### Viral RNA Quantification

A concentrated suspension of wild-type HIV-1 LAI strain produced from chronically infected MOLT-4 cells was used as the source of virus (10). As a quantification method for HIV-1, we used a nested competitive RT-PCR technique that we developed previously (10). Briefly, the internal competitor DNA consisted of an HIV-1 *env* sequence (nucleotide positions 6201 to 8805 according to NL4-3) (17) with deletion of positions 7119 to 7241 and addition of a T7 promoter (TAA TAC GAC TCA CTA TAG GGA GA) at the 5' terminus. Internal competitor RNA was synthesized from the competitor DNA with T7 RNA polymerase. The DNA and RNA were quantified by spectrophotometry and end point dilution followed by Poisson analysis of positive scores from nested PCR, as described previously. Using this method, viral load has been confirmed to be maintained consistently at approximately 10 copies/20  $\mu$ L.

### Determination of Buoyant Density of HIV-1 by Isopycnic Focusing

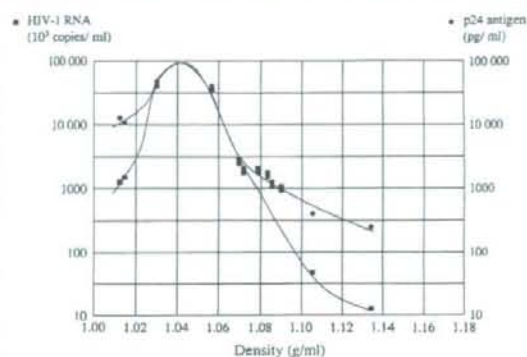
The HIV-1 LAI strain (0.2 mL) was mixed with 2.5 mL 65% Percoll or 2.5 mL 50% Pureception (final viral concentration  $1.15 \times 10^6$ /mL). After centrifugation at 16,400 g (Percoll) or 11,400 g (Pureception) for 20 minutes, aliquots of the postcentrifugation suspension (each approximately 0.25 mL) were fractionated beginning at the bottom of the tube. Mean specific gravity of each fraction was determined by weighing 100  $\mu$ L of each solution using a measuring micropipette. Viral concentration was determined by nested competitive RT-PCR, and p24 antigen was quantified with MiniVidas (Biomerieux, Marcy l'Etoile, France). Buoyant density of HIV-1 particles was determined from the solvent density corresponding to a peak of viral distribution.

### Preparation of Continuous Density Gradients with a Gradient Pump and Evaluation of Sedimentation Dynamics

Two pairs of solutions as described subsequently were mixed in a pump for column preparation (Bio-Rad, Philadelphia, PA) to prepare 3-mL continuous density gradients: either a mixture of 80% Percoll and Hanks solution or a mixture of 90% Pureception and sperm-washing medium. A 0.2-mL aliquot of the concentrated HIV-1 suspension was layered on top of the upper layer of the prepared density gradient. After centrifugation at 1,600 g for 5, 10, 20, and 40 minutes, aliquots of the postcentrifugation suspension (approximately 0.25 mL) were fractionated beginning at the bottom of the tube. Mean specific gravity was determined, and viral load in each fraction was quantified using the nested competitive RT-PCR technique.

FIGURE 1

Viral RNA load in each density fraction of Percoll. Fractions were collected from the bottom and analyzed for density, human immunodeficiency virus 1 (HIV-1) RNA (squares), and p24 (circles). The HIV-1 RNA and p24 amounts were plotted against the density of each fraction, using a semilogarithmic scale. Both HIV-1 RNA and p24 showed a single peak at the position representing a density of 1.042.



Kuji. Sedimentation kinetics of HIV-1. *Fertil Steril* 2008.

## RESULTS

### Buoyant Density in Percoll and Pureception

Viral RNA amounts, p24 antigen amounts, and medium density were determined in each of 12 fractions of a centrifuged mixture of HIV-1 LAI strain and 65% Percoll. Viral RNA and p24 antigen amounts were plotted against measured medium density using a semilogarithmic scale (Fig. 1). Assuming viral distribution curves to be normally distributed, distribution peaks of HIV-1 RNA and p24 antigen were calculated to exist at approximately 1.042 g/mL. Accordingly, the buoyant density of HIV-1 in Percoll was estimated to be 1.042 g/cm<sup>3</sup>. Data for Pureception are presented in Figure 2. The buoyant density of HIV-1 in Pureception was estimated to be 1.042 g/cm<sup>3</sup>, the same value as with Percoll. Viral distribution had a single peak in Percoll but showed two peaks in Pureception, with a small amount of virus in the higher-density fraction (bottom of the tube) in addition to the main peak.

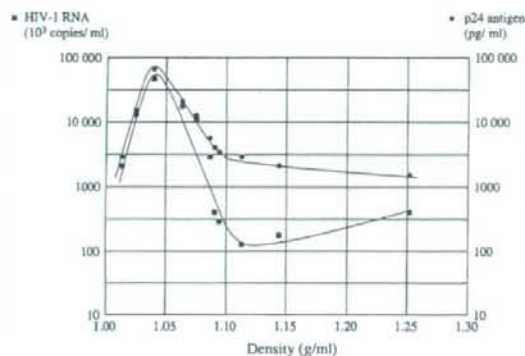
### Sedimentation Dynamics in Percoll and Pureception

High reproducibility was observed in the two continuous density gradients ranging from 0% to 90% Pureception and 0% to 80% Percoll. Linearity was maintained even after centrifugation at 1,600 g for 40 minutes (data not shown).

Using the continuous density gradients described, sedimentation dynamics of HIV-1 layered on the top of the upper layer of each gradient were investigated. Most HIV-1 particles were found in fractions with specific gravity less than 1.04, even after 40 minutes of centrifugation, in both continuous density gradient media (Fig. 3). In Pureception,

**FIGURE 2**

Viral RNA load in each density fraction of Pureception. Fractions were collected from the bottom and analyzed for density, human immunodeficiency virus 1 (HIV-1) RNA (squares), and p24 (circles). The HIV-1 RNA and p24 amounts were plotted against the density of each fraction, using a semilogarithmic scale. Amounts of p24 showed a single peak as for Percoll. The HIV-1 RNA amounts, however, showed two peaks: a small amount of virus at the higher-density position (the bottom of the centrifugation tube) in addition to the main peak.



Kuji. Sedimentation kinetics of HIV-1. Fertil Steril 2008.

however, small viral accumulations were observed at the bottom of the tube (data not shown), a finding absent with Percoll.

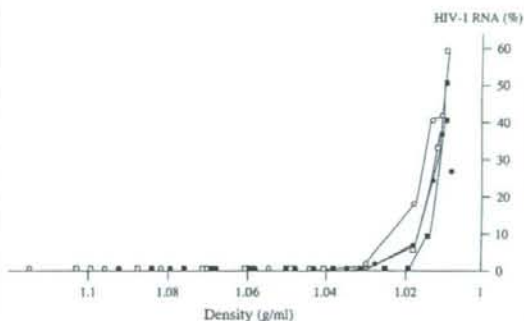
## DISCUSSION

When the male partner is HIV-1 positive, a female partner who is HIV-1 negative is estimated to incur a 0.1% to 0.2% risk of acquiring HIV-1 per act of unprotected intercourse (18). Thus, attempting to conceive naturally carries a serious risk to the uninfected female partner and to the child (19). Density-gradient centrifugation techniques can effectively eliminate HIV-1 from semen to reduce the risk of HIV-1 transmission in HIV-1-discordant couples wishing to have children (9, 10). Although Baccetti et al. (3) detected HIV-1 particles and HIV-1 nucleic acid in ejaculated washed sperm preparations from HIV-1-seropositive patients, other investigators noted total absence of HIV-1 particles and nucleic acid in washed sperm (1, 7, 20). Thus, separation of seminal fluid and cellular elements from sperm by washing techniques reduces the viral load of semen detected by PCR and RT-PCR. Consequently, several groups have achieved pregnancy successes without HIV-1 seroconversions by using sperm-washing methods (12, 13).

Separation of spermatozoa using density-gradient centrifugation is possible in part because spermatozoa are motile, un-

**FIGURE 3**

The human immunodeficiency virus 1 (HIV-1) viral load after centrifugation in Percoll and in Pureception (1,600 g). Concentrated HIV-1 suspension was layered on top of either Percoll or Pureception density gradient and centrifuged at 1,600 g for 5, 10, 20, or 40 minutes. Beginning at the bottom of the tube, each 0.25-mL aliquot was removed as a fraction and then analyzed. Viral load after centrifugation for 10 minutes (solid squares: Percoll; open squares: Pureception), and 40 minutes (solid circles: Percoll; open circles: Pureception) are shown. Most HIV-1 particles were present in fractions with specific gravity near or below 1.04, even after 40 minutes of centrifugation in continuous density gradients using both Percoll and Pureception. With Pureception, however, small viral accumulations were observed at the bottom of the tube (data not shown), a finding absent with Percoll.



Kuji. Sedimentation kinetics of HIV-1. Fertil Steril 2008.

like other particulates present; additionally, sedimentation velocities differ between spermatozoa, seminal plasma, lymphocytes, and free virus. Highly motile spermatozoa migrate more quickly than nonmotile constituents during density-gradient centrifugation, because centrifugal force orients them with head downward and tail upward (21). Because motility thus contributes importantly to separation, efficiency ordinarily is enhanced for spermatozoa owing to their motility. In contrast, for spermatozoa with impaired motility, especially those from HIV-1-positive men with infertility from factors such as oligozoospermia or asthenozoospermia, buoyant density as well as sedimentation velocity of the virus in sperm-washing media become the most important factors for separating virus from sperm. With poorly motile spermatozoa, density-gradient viral separation is likely to fail unless centrifugation-related factors are carefully considered.

In the present study, we investigated sedimentation dynamics of HIV-1 in two extensively used sperm-washing media, Percoll and Pureception. Percoll, a colloidal suspension of PVP-coated silica particles, has been used widely for sperm processing in assisted reproductive technology, offering



simplicity, rapidity, and excellent yields. In 1996, however, Percoll was withdrawn from clinical use in humans because of concern over possible endotoxin contamination. Pureception, a colloidal suspension of silane-coated silica particles developed as a substitute, has been shown to be effective in recovering motile sperm by several studies comparing it with Percoll, and it is now used worldwide (22–26).

The buoyant density for HIV-1 in a linear sucrose gradient was reported to be 1.16 g/mL (27), which differs from the buoyant density of 1.04 g/mL obtained in the present experiment with both sperm-washing density gradient media, Percoll and Pureception. In isopycnic focusing, buoyant densities of particles can vary considerably according to the composition of the density gradient media used, reflecting differences in osmolarity of the medium (28). We therefore took care to use the same density gradient media actually used for sperm washing in determining the buoyant density of HIV-1. This value proved to be equal between the two sperm washing media, Percoll and Pureception, probably because both consist mainly of silica gel. Their osmotic pressures were kept equal in view of their having a common use, processing of spermatozoa.

We also examined the sedimentation velocity of HIV-1 in continuous density gradients made of Percoll and Pureception. These continuous-gradient columns, prepared with a gradient pump, demonstrated high reproducibility and post-centrifugation stability. In clinical settings, use of discontinuous density gradients is quite common, whereas continuous density gradients are rarely used, because highly specialized equipment and personnel are required to prepare reproducible gradients. However, with discontinuous density gradients, virus may be trapped at the interface between densities and the sedimentation rate of the virus also may change as a result of viral aggregation—especially when high concentrations of virus are applied, as in the present study. For that reason, we used continuous density gradients for determination of the distribution of viral particles among the sedimentation fractions. High concentrations of HIV-1 were layered on the upper surface of the continuous density gradient before centrifugation. Even after centrifugation at 1600 g for 40 minutes, almost all HIV-1 virus particles remained in the superficial fractions where density was near or less than 1.042, the determined buoyant density of HIV-1. This confirmed that the sedimentation velocity of HIV-1 was very low in continuous density gradients made up from either Percoll or Pureception.

Interestingly, minute amounts of virus were found to be clustered at the bottom of the Pureception gradient tube but not the Percoll gradient tube. The reason for this difference remains unknown, but one possible explanation might involve a difference in silica particle size between Percoll and Pureception. The average diameter of Percoll particles is about 17.2 nm, and the size of the particles in Pureception before silane coating is about 15 nm; the density-gradient particles in Percoll would appear to be slightly larger than those in Pureception. Another possible explanation might

involve differences in the substances coating the silica particles. Silane (in Pureception) might exert slightly less friction against various particles than PVP (in Percoll). In fact, the recovery rate of spermatozoa has been reported to be greater using Pureception than using Percoll (22). The decreased friction in Pureception might permit small HIV-1 aggregates to form.

Effectiveness of clinical management of HIV-1—serodiscordant couples using sperm washing followed by a swim-up technique is presently under investigation. After carrying out artificial insemination in more than 300 cases, Semprini et al. (12) reported that transmission of infection was prevented successfully in all subjects. In contrast, another study found transmission of infection in some cases where the semen was subjected only to a washing procedure (29). Although several problems remain to be solved, the American Society for Reproductive Medicine recommended in 2004 that procedures for HIV-1-discordant couples wanting a child can be performed, but only at institutions able to provide the most effective methods of sperm preparation as well as the rigorous testing and treatment necessary to minimize the chance of HIV-1 transmission to partner and offspring (30).

In conclusion, we investigated the buoyant density of HIV-1 and dynamic changes in the sedimentation pattern of free HIV-1 in both Percoll and Pureception media for “sperm washing.” We found very high efficiency of free virus removal using either medium for density-gradient centrifugation. However, a minute quantity of virus was found at the bottom of the gradient tube in addition to the virus retained in overlying fractions when Pureception was used as the medium. Accordingly, washing procedures used clinically must be assessed individually in terms of specific type of density gradient medium.

*Acknowledgements:* The authors acknowledge the assistance of Ms. Kazuyo Nakamura, B.A. in preparing the manuscript.

## REFERENCES

1. Quayle AJ, Xu C, Mayer KH, Anderson DJ. T Lymphocytes and macrophages, but not motile spermatozoa, are a significant source of human immunodeficiency virus in semen. *J Infect Dis* 1997;176:960–8.
2. Baccetti B, Benedetto A, Burrini AG, Collodel G, Elia C, Piomboni P, et al. HIV particles detected in spermatozoa of patients with AIDS. *J Submicrosc Cytol Pathol* 1991;23:339–45.
3. Baccetti B, Benedetto A, Burrini AG, Collodel G, Ceccarini EC, Crisa N, et al. HIV-particles in spermatozoa of patients with AIDS and their transfer into the oocyte. *J Cell Biol* 1994;127:903–14.
4. Scofield VL, Rao B, Broder S, Kennedy C, Wallace M, Graham B, et al. HIV interaction with sperm. *AIDS* 1994;8:1733–6.
5. Bagasra O, Farzadegan H, Seshamma T, Oakes JW, Saah A, Pomerantz RJ. Detection of HIV-1 proviral DNA in sperm from HIV-1-infected men. *AIDS* 1994;8:1669–74.
6. Gobert B, Amiel C, Tang JQ, Barbarino P, Bene MC, Faure G. CD4-like molecules in human sperm. *FEBS Lett* 1990;261:339–42.
7. Lasheeb AS, King J, Ball JK, Curran R, Barratt CL, Afnan M, et al. Semen characteristics in HIV-1 positive men and the effect of semen washing. *Genitourin Med* 1997;73:303–5.
8. Nuovo GJ, Becker J, Burk MW, Margiotta M, Fuhrer J, Steighigel RT. In situ detection of PCR-amplified HIV-1 nucleic acids in lymph nodes and

- peripheral blood in patients with asymptomatic HIV-1 infection and advanced-stage AIDS. *J Acquir Immune Defic Syndr* 1994;7:916-23.
9. Kim LU, Johnson MR, Barton S, Nelson MR, Sontag G, Smith JR, et al. Evaluation of sperm washing as a potential method of reducing HIV transmission in HIV-discordant couples wishing to have children. *AIDS* 1999;13:645-51.
  10. Hanabusa H, Kuji N, Kato S, Tagami H, Kaneko S, Tanaka H, et al. An evaluation of semen processing methods for eliminating HIV-1. *AIDS* 2000;14:1611-6.
  11. Semprini AE, Levi-Setti P, Bozzo M, Ravizza M, Taglioretti A, Sulpizio P, et al. Insemination of HIV-negative woman with processed semen of HIV-positive partners. *Lancet* 1992;340:1317-9.
  12. Semprini AE, Fiore S, Pardi G. Reproductive counselling for HIV-discordant couples. *Lancet* 1997;349:1401-2.
  13. Marina S, Marina F, Alcolea R, Exposito R, Huguot J, Nadal J, et al. Human immunodeficiency virus type 1-serodiscordant couples can bear healthy children after undergoing intrauterine insemination. *Fertil Steril* 1998;70:35-9.
  14. Weigel MM, Gentili M, Beichert M, Friese K, Sonnenberg-Schwan U. Reproductive assistance to HIV-discordant couples—the German approach. *Eur J Med Res* 2001;6:259-62.
  15. Pena JE, Thornton MH Jr, Sauer MV. Reversible azoospermia: anabolic steroids may profoundly affect human immunodeficiency virus-seropositive men undergoing assisted reproduction. *Obstet Gynecol* 2003;101:1073-5.
  16. Kaneko S, Sato H, Kobanawa K, Oshio S, Kobayashi T, Iizuka R. Continuous-step density gradient centrifugation for the selective concentration of progressively motile sperm for insemination with husband's semen. *Arch Androl* 1987;19:75-84.
  17. Adachi A, Gendelman HE, Koenig S, Folks T, Willey R, Rabson A, et al. Production of acquired immunodeficiency syndrome-associated retrovirus in human and nonhuman cells transfected with an infectious molecular clone. *J Virol* 1986;59:284-91.
  18. Mastro TD, de Vincenzi I. Probabilities of sexual HIV-1 transmission. *AIDS* 1996;10(Suppl A):S75-82.
  19. Mandelbrot L, Heard I, Henrion-Geant E, Henrion R. Natural conception in HIV-negative women with HIV-infected partners. *Lancet* 1997;349:850-1.
  20. Pudney J, Nguyen H, Xu C, Anderson DJ. Microscopic evidence against HIV-1 infection of germ cell or attachment to sperm. *J Reprod Immunol* 1999;44:57-77.
  21. Gorus FK, Pipeleers DG. A rapid method for the fractionation of human spermatozoa according to their progressive motility. *Fertil Steril* 1981;35:662-5.
  22. Perez SM, Chan PJ, Patton WC, King A. Silane-coated silica particle colloid processing of human sperm. *J Assist Reprod Genet* 1997;14:388-93.
  23. Claassens OE, Menkveld R, Harrison KL. Evaluation of three substitutes for Percoll in sperm isolation by density gradient centrifugation. *Hum Reprod* 1998;13:3139-43.
  24. Chen MJ, Bongso A. Comparative evaluation of two density gradient preparations for sperm separation for medically assisted conception. *Hum Reprod* 1999;14:759-64.
  25. Soderlund B, Lundin K. The use of silane-coated silica particles for density gradient centrifugation in in-vitro fertilization. *Hum Reprod* 2000;15:857-60.
  26. Mousset-Simeon N, Rives N, Masse L, Chevallier F, Mace B. Comparison of six density gradient media for selection of cryopreserved donor spermatozoa. *J Androl* 2004;25:881-4.
  27. Cimarelli A, Sandin S, Hoglund S, Luban J. Basic residues in human immunodeficiency virus type 1 nucleocapsid promote virion assembly via interaction with RNA. *J Virol* 2000;74:3046-57.
  28. Pertoft H. Fractionation of cells and subcellular particles with Percoll. *J Biochem Biophys Methods* 2000;44:1-30.
  29. Centers for Disease Control (CDC). Epidemiologic notes and reports: HIV-1 infection and artificial insemination with processed semen. *MMWR Morb Mortal Wkly Rep* 1990;249:255-6.
  30. Ethics Committee of the American Society for Reproductive Medicine. Human immunodeficiency virus and infertility treatment. *Fertil Steril* 2004;82(suppl 1):S228-31.



## Increasing genetic diversity of hepatitis C virus in haemophiliacs with human immunodeficiency virus coinfection

Yasuhito Tanaka,<sup>1</sup> Kousuke Hanada,<sup>2</sup> Hideji Hanabusa,<sup>3</sup> Fuat Kurbanov,<sup>1</sup> Takashi Gojbori<sup>2</sup> and Masashi Mizokami<sup>1</sup>

Correspondence  
Yasuhito Tanaka  
ytanaka@med.nagoya-cu.ac.jp

<sup>1</sup>Department of Clinical Molecular Informative Medicine, Nagoya City University Graduate School of Medical Sciences, Kawasumi, Mizuho, Nagoya 467-8601, Japan

<sup>2</sup>National Institute of Genetics, Yata 1111, Mishima, Shizuoka, Japan

<sup>3</sup>Ogikubo hospital, Tokyo, Japan

Patients with inherited bleeding disorders who received clotting factor concentrates before 1987 have high rates of hepatitis C virus (HCV) or HCV/human immunodeficiency virus (HIV) infection. To determine whether the persistent nature of HIV affects the genetic diversity of HCV by less selective pressure through the immunosuppression of HIV/HCV-coinfected patients, both the change of genetic diversity and selective pressure were examined in the HCV envelope genes (E1 and E2) of 325 genotype 1a subclones from eight HIV-positive and five HIV-negative patients with two time points (more than 6 years apart). To infer the genetic diversity of HCV in each patient, we used two approaches. One method was to estimate the difference of total evolutionary distances in the phylogenetic tree between the two time points, and another was to estimate the changes of genetic diversity along the time based on the coalescence theory. The two results indicate that the HIV-positive group has significantly more diverse population structure than the HIV-negative group. A comparative analysis of the synonymous and non-synonymous substitutions found that the HIV-positive group was subject to less selective pressure than the HIV-negative group. In conclusion, HIV-positive patients would have a more diversified HCV population than HIV-negative patients due to less selective pressure from the immune system.

Received 6 March 2007  
Accepted 3 May 2007

### INTRODUCTION

Increased rates of progression to end-stage liver disease, mortality and reduced treatment response rates have been well documented in haemophiliac and other groups of chronic hepatitis C virus (HCV) carriers with human immunodeficiency virus (HIV) coinfection (Bica *et al.*, 2001; Goedert *et al.*, 2002; Braitstein *et al.*, 2004). Although the mechanism of liver disease progression in HIV-infected patients remains unclear, one of the important roles is assigned to immunosuppression (Goedert *et al.*, 2002).

The estimated HCV virion half-life time was, on average, 2.7 h with pre-treatment production and clearance of  $10^{12}$  virions per day (Neumann *et al.*, 1998). Such a high rate of HCV replication, combined with lack of an error correction mechanism, results in the development of genetically diverse clones in a patient. The genetic diversity of HCV has provided critical insights into short-term outcomes, including early spontaneous viral clearance (Farci *et al.*, 2000), interferon-associated viral clearance (Farci *et al.*,

2002; Pawlotsky *et al.*, 1999) and HCV emergence following liver transplantation (Lyra *et al.*, 2002). To infer the genetic diversity of HCV in a patient, we applied two approaches. One method simply assumed that the genetic diversity of HCV is of different divergence of synonymous distance between two time points. The other method applied to coalescent analysis of genetic diversity along the time, assuming that the genetic diversity of HCV represents a heterogeneous viral population in a given carrier. To evaluate the influence on the HCV evolution exerted by the immunosuppression during persistent HIV coinfection, we examined a cohort of HCV carriers, comparing the HIV-positive and -negative groups.

Determination of the antigen-recognition regions associated with HCV-specific immune positive selection is important for understanding selective pressures underlying the evolution of HCV as well as putative therapeutic targets. In this study, we evaluated the genetic diversity of HCV and determined genomic regions associated with positive selection by comparative analysis of selective forces between HIV-positive and -negative groups in a cohort of haemophilia patients followed for more than 6 years.

The GenBank/EMBL/DDBJ accession numbers for the sequences reported in this study are AB245555–AB245873.

## METHODS

**Selection of patients.** The patients enrolled in the present study were a subset of a well-characterized cohort of 166 patients with haemophilia who had received non-heated plasma-derived coagulation products before 1987 and had been observed regularly since 1995 at Ogikubo hospital (Tokyo, Japan). Plasma samples from patients with known HCV and HIV serological status were stored at  $-80^{\circ}\text{C}$ . Of these patients, 57 were positive and 109 were negative for anti-HIV. After exclusion of HCV-RNA-negative and interferon-treated patients, and those with a mixture or shift in HCV subtypes during the follow-up, 13 HCV-1a-RNA-positive patients (eight HIV-positive and five HIV-negative patients) were selected at random for this study. The study protocol conformed to the 1975 Declaration of Helsinki and was approved by the Ethics Committees of each institution. Every patient gave written informed consent to participate in the virological research.

**Laboratory tests.** Laboratory evaluation included complete blood cell count and serum transaminases [alanine aminotransferase (ALT)], CD4<sup>+</sup> cell counts were examined by fluorescence-activated cell sorting at SRL Inc. (Tokyo, Japan). Serum HCV-RNA levels and HIV-RNA levels were measured by a commercial PCR assay (Amplicor HIV-1 Monitor and Amplicor HCV monitor; Roche Diagnostics). The detection limits of PCR for HCV-RNA and HIV-RNA were 500 IU ml<sup>-1</sup> [0.5 kilo international unit (KIU) ml<sup>-1</sup>] and 50 copies ml<sup>-1</sup>, respectively.

**HCV-RNA isolation and amplification from the core, E1 and E2 regions.** Nucleic acids were extracted from serum samples using a SepaGene RV-R Nucleic Acid Extracting kit (Sanko Junyaku) in accordance with the manufacturer's protocol. Viral RNA was reverse-transcribed to cDNA using SuperScript II RNase H<sup>-</sup> Reverse Transcriptase (Invitrogen) and random hexamer primer (Takara Shuzo) as described previously (Ohno *et al.*, 1997).

Partial core, E1 and E2 fragments were amplified by using PCR with primers as described previously (Tanaka *et al.*, 2002). To reduce the number of artificial substitutions arising during PCR, Platinum Pfx DNA Polymerase (Invitrogen) with a very high fidelity was used.

**Cloning and sequencing of cDNA.** The amplified products were ligated into pCR-Blunt II-TOPO Vector and used to transform DH5- $\alpha$  high-efficiency competent cells according to the manufacturer's protocol (Invitrogen). The plasmid DNA was purified using the QIAprep Spin Miniprep kit (Qiagen) and the presence of the inserts confirmed by digestion with EcoRI. Sequencing was performed on more than 10 clones per patient at the baseline (1995–1997) and the end point (2002–2003). All clones were sequenced with Prism Big Dye (Applied Biosystems) in an ABI 3100 DNA automated sequencer.

**Construction of phylogenetic trees.** Nucleotide sequences of HCV were aligned by using the program CLUSTAL\_X and molecular evolutionary analyses were conducted using Molecular Evolutionary Genetic Analysis software (MEGA version 3.0; Kumar *et al.*, 2001). The MEGA algorithms were used to calculate the mean Tamura–Nei pairwise distance for all clones as well as a matrix of Tamura–Nei pairwise distances for each patient. To confirm the reliability of the phylogenetic tree, bootstrap resampling tests were performed 1000 times.

**Genetic diversity of HCV over a time course.** Two approaches were used to infer the genetic diversity of HCV in each patient. In the first approach, total evolutionary distances among a heterogeneous viral population were compared between the baseline and end point for each patient in the phylogenetic tree. The phylogenetic tree of genetic diversity was constructed by using the maximum-likelihood (ML) method and the ancestral sequence was inferred at every node

using the ML method (Yang *et al.*, 1995). As the evolutionary distance in each branch, the number of synonymous substitutions per synonymous site (synonymous distance) was estimated by the modified Nei–Gojobori method. Total synonymous distances were assumed to represent the genetic diversity of a heterogeneous viral population in each patient.

The other approach is the coalescence theory based on estimation of the genetic diversity. A consensus sequence based on the sequences of all HCV clones isolated from each patient was used as an outgroup to locate the position of the root in each phylogenetic tree. The topology of the phylogenetic tree was estimated by the neighbour-joining method (PHYLIP). Based on the topology, we constructed the phylogenetic tree and inferred the evolutionary rate by the ML method under the premise of the molecular clock (TipDate) (Rambaut, 2000). Based on the trees and the evolutionary rates estimated by TipDate, the coalescent analysis of genetic diversity was conducted for each patient using the Genie v3.5 software (Pybus *et al.*, 2001; Pybus & Rambaut, 2002). In brief, time  $t$  was transformed to year using the HCV molecular evolutionary rate, assuming the sample-collection time to be the present. Function  $N(t)$  (effective numbers of HCV infections through time) was estimated by the ML method to infer the genetic diversity of HCV (Pybus & Rambaut, 2002). Although there are several models to infer  $N(t)$ , the best-fit model was different among patients. Therefore, we chose a simplified model in which the genetic diversity was assumed to be exponentially increased over time (expansion model).

**Identification of positively selective regions.** Positively selected regions were identified using the modified method of Suzuki & Gojobori (2001). In brief, a phylogenetic tree of sequences from HCV clones was reconstructed in each patient by the ML method. The ancestral sequence was inferred at every node in the phylogenetic tree using the ML method (Yang *et al.*, 1995). Then, synonymous and non-synonymous substitutions throughout the phylogenetic tree were estimated in each branch for each codon site. Here, to see the differences in selective pressure for HCV between the HIV-positive and -negative groups, we independently summed the total numbers of synonymous ( $N_s$ ) and non-synonymous ( $N_n$ ) substitutions occurring at each codon site of the HCV clones from either eight patients infected with HIV or five patients without HIV infection. The mean numbers of synonymous ( $C_s$ ) and non-synonymous ( $C_n$ ) sites were calculated for each codon site by the modified Nei–Gojobori method. The genetic distance of synonymous ( $d_s$ ) and non-synonymous ( $d_n$ ) was calculated as  $N_s/C_s$  and  $N_n/C_n$ , respectively. Although the ratio  $d_n/d_s$  is usually used for estimating selective pressure, we used  $(d_n + 0.5)/(d_s + 0.5)$  ratio instead in the present study, because no synonymous substitution was found in several codon sites. The ratio was calculated along with the sequence by the sliding-window analysis. Each window size consisted of three codons.

## RESULTS

### Comparison of clinical characteristics between HCV patients with and without HIV infection

When we compared clinical data between HCV patients with HIV (HIV-positive group) and without HIV (HIV-negative group), there were no significant differences of mean age, sex, putative duration of HCV infection or mean peak ALT levels (116 vs 146) (Table 1). Changes of ALT levels also were not different between these two groups. Mean peaks of HCV-RNA levels in the HIV-positive group ( $2300 \pm 668$  KIU ml<sup>-1</sup>), however, were significantly higher than those in the HIV-negative group ( $936 \pm 423$ ,  $P =$



**Table 1.** Clinical characteristics among HCV patients in this study

All patients are male. HCV genotype of all patients is 1a. LC, Liver cirrhosis; ALT, alanine aminotransferase; NT, not tested; +, positive; -, negative.

ID	Age	Putative date of HCV infection	LC	HIV	AIDS	HIV-RNA (copies ml <sup>-1</sup> )	CD4 at baseline (μl <sup>-1</sup> )	HCV-RNA (KIU ml <sup>-1</sup> )			ALT (U l <sup>-1</sup> )	
								Range	Peak	Increase ×2	Range	Increase ×2
NT211	29	1982	-	+	+	130 000	20	130-2100	2100	yes	20-156	yes
GM248	39	1986	-	+	-	23 000	110	290-1200	1200	yes	34-96	yes
OT33	34	1982	-	+	-	2300	286	170-2000	2000	yes	40-43	no
HH127	33	1980-1982	-	+	-	22 000	270	330-3200	3200	yes	27-168	yes
TA92	32	1984	-	+	-	98 000	271	1300-2900	2900	yes	29-34	no
KY48	31	1980-1983	-	+	-	55 000	242	730-2700	2700	yes	66-213	yes
NK112	28	1982	+	+	+	100 000	27	2300-2600	2600	yes	16-28	no
YY321	27	1987	-	+	+	95 000	35	1200-1700	1700	no	181-186	yes
KK202	19	1987	-	-	-	NT	NT	310-1600	1600	yes	21-41	no
KN201	45	1982	+	-	-	NT	NT	300-710	710	no	38-98	no
TS246	20	1984	-	-	-	NT	NT	230-1000	1000	yes	27-37	no
SH265	20	1985	-	-	-	NT	NT	340-470	470	no	130-470	yes
ST251	26	1984	-	-	-	NT	NT	590-900	900	no	38-83	yes

0.0019), which is consistent with previous reports (Eyster *et al.*, 1994). Additionally, seven of eight patients in the HIV group had HCV-RNA elevation more than twice during follow-up, whereas only two patients in the HIV-negative group had HCV-RNA elevation.

For the eight HCV patients in the HIV-positive group, HIV-RNA and CD4 are shown in Table 1. Three of the patients had already developed AIDS and had very low CD4 counts (20, 27, 35 μl<sup>-1</sup>), and the remaining five patients with HIV also had relatively low CD4 levels (110-286) at the baseline (1995-1997) before initiating highly active anti-retroviral therapy (HAART). Thereby, all HIV-infected patients studied were considered to be in an immunity-suppressed condition. Four patients with a CD4 count less than 200, including the three AIDS patients, received anti-HIV treatments.

#### Long-term intra-host diversity of HCV evaluated on distinct genomic regions

It has been shown previously that the genetic diversity of HCV changes in an oscillatory manner during the natural course of the infection (Devereux *et al.*, 1997). Taking into account that the genetic diversity of HCV analysed at a single time point might not accurately reflect the dynamic profile of the population over time, we have examined 26 serum samples collected from 13 patients at two distinct time points with intervals of at least 6 years (6-8 years). At least 11 HCV clones were isolated from a single patient at the baseline (1995-1997) and at the end point (2002-2003) of the follow-up. Overall, 325 HCV clones were thus isolated and analysed. All of them belonged to genotype 1a. Phylogenetic relation of the HCV clones isolated from all patients is shown in Fig. 1. Assuming that HCV is composed of a heterogeneous viral population, which is evolving throughout time in a given host (carrier), we

aimed to estimate the size and heterogeneity of the population. Two different methods were used to attain this aim.

First, we directly compared the genetic diversity of a heterogeneous viral population between the two time points. To do that, we estimated totals (for all patients in each of the two groups) of intra-host synonymous distances at each of the two time points. This estimation was done independently in both E1 and E2 genomic regions (Fig. 2). The increased difference from the baseline to the end point between the HIV-positive and HIV-negative groups was tested by the regression analysis, and the genetic diversity of the HIV-positive group is significantly higher than that of the HIV-negative group ( $P=0.043$ ).

Second, the coalescent analysis of genetic diversity of HCV was conducted for each patient. Further, mean curves of the effective numbers of HCV infections were compared between HIV-positive and -negative groups (Fig. 3). Although the estimated mean number was initially relatively lower in the HIV-positive group, the rapid change to exponential growth, was observed several years after HIV infection in this group, whereas in the HIV-negative group, the effective number was gradually increasing throughout the period of time. The difference of exponential growth is significant ( $P=0.04$ ). Hence, the result obtained by either method indicated the HIV-positive group to have higher genetic diversity of the heterogeneous viral population than the HIV-negative group, suggesting that this was due to the exposure of HIV infection.

#### Putative positively selective regions in the E1 and E2 regions

Since the higher genetic diversity of HCV was observed in HIV-positive patients, we further examined genetic evi-

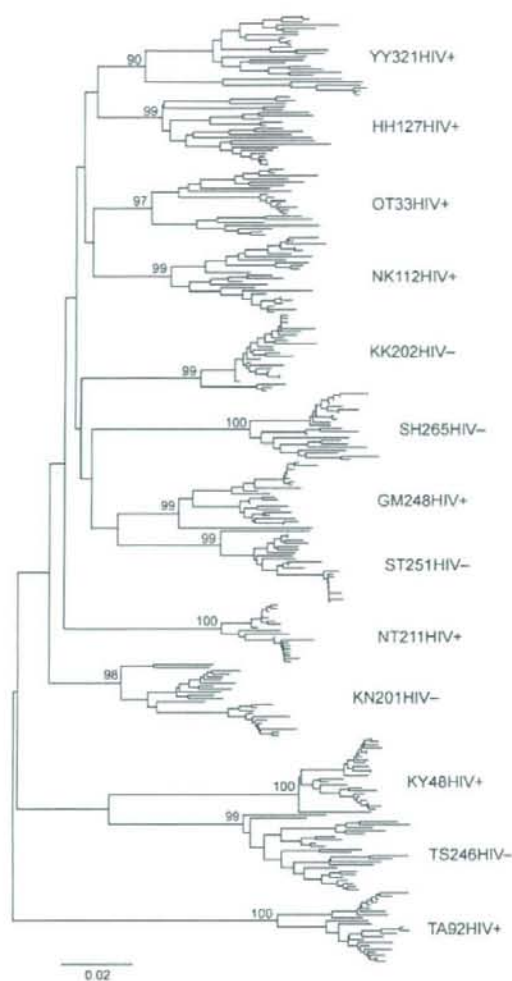


**Fig. 1.** A phylogenetic tree of E1 and E2 regions of the 325 HCV clones isolated from 13 patients. The significant phylogenetic cluster was observed in each of the eight HIV-positive (HIV+) and five HIV-negative (HIV-) patients. Numbers at nodes indicate bootstrap values of 1000 replications.

dence of the selective immune pressure in both groups. Selective immune pressure was estimated in each, E1 and E2, gene. Some differences were observed between the HIV-positive and -negative groups (Table 2, Fig. 4). Immune epitopes (11 aa segments in the E1 and 5 aa segments in the E2 region) that were observed only in the HIV-negative group might have relatively weak antigenicity. Some of the segments were previously recognized as HCV-specific potential immunogenic targets such as

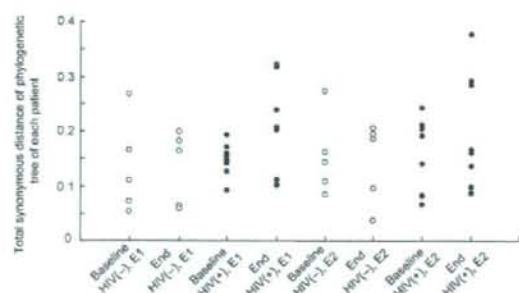


**Fig. 2.** Total synonymous distances of the phylogenetic tree of each time point. *y*-axis indicates total synonymous distance of the phylogenetic tree constructed by the sequences isolated at each time point. *x*-axis indicates two time points [baseline and end point (End)] and two groups [HIV-positive (HIV+) and -negative (HIV-)]. Each dot represents a patient.

cytotoxic T lymphocyte (CTL) epitopes (URL: [http://hcv.lanl.gov/content/immuno/tables/ctl\\_summary.html](http://hcv.lanl.gov/content/immuno/tables/ctl_summary.html)), indicating that the positively selected segments estimated in the present study are associated with the immune response. On the other hand, positively selected segments around the hypervariable region (HVR1) regardless of HIV infection should have strong antigenic epitopes, suggesting little influence of the HIV coinfection on the natural immune selection targeting this region.

## DISCUSSION

A previous meta-analysis showed a significantly elevated relative risk of severe liver disease in patients coinfecting

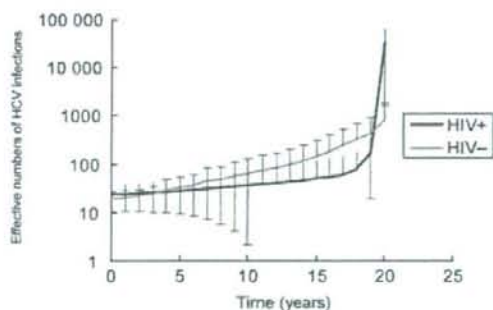


**Fig. 3.** The mean effective numbers of HCV infections in HIV-positive (HIV+) and -negative (HIV-) groups over the years from the baseline. Two lines indicate the dynamics of the mean effective numbers of HCV infections (*y*-axis) estimated in the E2 region and the bars indicate standard deviations. *x*-axis indicates number of years from the end point.